Published in final edited form as:
Basic Res Cardiol. 2011 March ; 106(2): 273–286. doi:10.1007/s00395-010-0146-8.

Central TNF inhibition results in attenuated neurohumoral excitation in heart failure: a role for superoxide and nitric oxide

Anuradha Guggilam, **Jeffrey P. Cardinale**, **Nithya Mariappan**, **Srinivas Sriramula**, **Masudul Haque**, and **Joseph Francis**
Comparative Biomedical Sciences, School of Veterinary Medicine, Louisiana State University, 1909 Skip Bertman Drive, Baton Rouge, LA 70803, USA

Joseph Francis: jfrancis@lsu.edu

Abstract

This study examined the effect of central tumor necrosis factor-alpha (TNF) blockade on the imbalance between nitric oxide and superoxide production in the paraventricular nucleus (PVN) and ventrolateral medulla (VLM), key autonomic regulators, and their contribution to enhanced sympathetic drive in mice with congestive heart failure (CHF). We also used a TNF gene knockout (KO) mouse model to study the involvement of TNF in body fluid homeostasis and sympathoexcitation in CHF. After implantation of intracerebroventricular (ICV) cannulae, myocardial infarction (MI) was induced in wild-type (WT) and KO mice by coronary artery ligation. Osmotic mini-pumps were implanted into one set of WT + MI/Sham mice for continuous ICV infusion of Etanercept (ETN), a TNF receptor fusion protein, or vehicle (VEH). Gene expressions of neuronal nitric oxide synthase (NOS) and angiotensin receptor-type 2 were reduced, while those of inducible NOS, Nox2 homologs, superoxide, peroxynitrite and angiotensin receptor-type 1 were elevated in the brainstem and hypothalamus of MI + VEH. Plasma norepinephrine levels and the number of Fos-positive neurons were also increased in the PVN and VLM in MI + VEH. MI + ETN and KO + MI mice exhibited reduced oxidative stress, reduced sympathoexcitation and an improved cardiac function. These changes in WT + MI were associated with increased sodium and fluid retention. These results indicate that elevated TNF in these autonomic regulatory regions of the brain alter the production of superoxide and nitric oxide, contributing to fluid imbalance and sympathoexcitation in CHF.

Keywords

Tumor necrosis factor; Congestive heart failure; Paraventricular nucleus; Rostral ventrolateral medullary nucleus; Sympathoexcitation; Oxidant stress

Introduction

Congestive heart failure (CHF) is a complex phenomenon characterized by the adverse activation of neurohormones such as norepinephrine (NE) and angiotensin II (AngII), and immune peptides including pro-inflammatory cytokines (PICs) such as tumor necrosis

Correspondence to: Joseph Francis, jfrancis@lsu.edu.

A. Guggilam and J. P. Cardinale have contributed equally to this work.

Electronic supplementary material The online version of this article (doi:10.1007/s00395-010-0146-8) contains supplementary material, which is available to authorized users.

Conflict of interest None declared.

factor-alpha (TNF), interleukin (IL)-1β and IL-6. Studies show that elevated circulating cytokines directly correlate with deteriorating NYHA functional classes of heart failure [41, 42]. The most well studied of these PICs is TNF, which can be cardio-protective [24, 26], but more often is implicated in the maladaptive left ventricular (LV) remodeling observed in CHF [5, 8, 21, 24, 27, 40]. TNF contributes to cardiac remodeling by provoking myocyte hypertrophy and apoptosis [25], ultimately leading to contractile dysfunction [2, 5, 40]. Furthermore, recent studies underscore the importance of brain site specific increases in PIC expression in the increased sympathoexcitation observed in CHF [16, 17].

Following an acute myocardial infarction (MI), elevated PICs are primarily transported into the hypothalamus and brainstem via the circumventricular organs, areas that lack a well-formed blood brain barrier (BBB) [33], through transcytosis [1], and/or increased BBB damage/vascular permeability by AngII or PICs [7, 11, 15, 51]. Circulating AngII and PICs are also major activators of microglial cells, astrocytes and macrophages [13, 34, 39, 47], which consequently produce more PICs, thereby propagating a vicious cycle [38]. These PICs are distributed throughout the brain, but more so in the hypothalamus and brainstem, regions that regulate sympathetic outflow to various cardiovascular and fluid homeostatic organ systems [16, 17, 20]. The hypothalamic paraventricular nucleus (PVN) and the ventrolateral medullary regions (VLM) of the brainstem are major central nervous system (CNS) sites that regulate thirst, salt appetite and sympathetic outflow. Intracerebroventricular (ICV) administration of AngII increases thirst and salt appetite, largely through elevated reactive oxygen species (ROS) production [52]. This AngII-induced ROS in the VLM plays a key role in the modulation of sympathetic nerve activity (SNA) and cardiovascular function [14, 32]. AngII type-1 receptor (AT1R) blockade in the PVN and rostral VLM (RVLM) attenuated ROS generation [18], contributing to decreased SNA in CHF. These studies emphasize the importance of central AngII-induced ROS on cardiovascular function. Additionally, there is an existent cross-talk between AngII, PICs and ROS in the brain in CHF [17]. Our previous studies showed that in CHF, the increase in TNF in the PVN is associated with elevated expression of NADPH oxidase subunits, the primary source of superoxide anions ($O_2^{\cdot-}$) [16], and intimately involves the actions of the renin–angiotensin system (RAS) [17]. Moreover, blockade of PVN $O_2^{\cdot-}$ completely abolished the increased SNA observed in CHF [18]. However, the importance of central TNF in increased sympathoexcitation is not completely understood.

Based upon the preceding observations, we hypothesized that elevated TNF in the PVN and RVLM alters $O_2^{\cdot-}$ and nitric oxide (NO) production, possibly through AT1R activation, thereby contributing to sympathoexcitation in CHF. This hypothesis was explored using two approaches: (1) chronic central TNF blockade with etanercept (a human recombinant TNF receptor fusion protein that competitively binds with TNF and prevents TNF from binding its receptor) in CHF mice and (2) a conventional TNF gene knockout mouse model to study the role of TNF in body fluid homeostasis and sympathoexcitation in CHF. We also explored the interaction between $O_2^{\cdot-}$ and NO in the PVN and RVLM and its contribution towards sympathoexcitation in CHF. The results of this study provide insight into the mechanisms that induce sympathoexcitation and disease progression in the failing heart.

Methods

Please see the online data supplement for additional details of the surgical and experimental methods mentioned here.

Mice

Male TNF knockout (KO; B6;129S-*Tnf*^{tm1Gkl}/), and wild-type (WT; B6129SF2/J) mice (Jackson Laboratory, ME) between 12–16 weeks of age were used in this study. Mice were housed in a light- (12 h light–dark cycle) and temperature-controlled (23 ± 2°C) room with standard chow and water provided ad libitum. All surgical procedures were performed at Louisiana State University School of Veterinary Medicine and carried out in accordance with the regulations of the Louisiana State University Animal Care and Use Committee, conforming to the *Guide for the Care and Use of Laboratory Animals* published by the US National Institutes of.

Drugs

Etanercept (ETN; Enbrel; Amgen and Wyeth Pharmaceuticals; Collegeville, PA, USA), was dissolved in artificial cerebrospinal fluid (aCSF) for ICV infusion. The dose used in this study was optimized by preliminary experiments conducted in our lab.

Experimental protocol and surgical procedures

The study was conducted under two protocols.

Protocol I—To study the effect of central TNF blockade on sympathoexcitation, WT mice were implanted with ICV cannulae into their right lateral cerebral ventricle. After a 1-week recovery, mice underwent either coronary artery ligation (CAL) to induce MI or sham (WT + Sham, $n = 15$) surgery. While still anesthetized, a 28-day osmotic mini-pump (Alzet) was implanted subcutaneously into each mouse and connected to the lateral ventricle cannula for continuous infusion (0.11 μl/h) of ETN (5 μg/kg/h) (MI + ETN, $n = 10$; Sham + ETN, $n = 10$) or aCSF as vehicle (VEH; VEH + MI, $n = 11$) over a 4-week treatment interval. As tissue gene, protein, echocardiographic and morphological results from Sham + ETN were unchanged from WT + Sham mice, these findings were not reported in this study.

Protocol II—KO and WT mice were used in this study to delineate the role of TNF on sodium and fluid retention and subsequent sympathoexcitation in CHF. After 1-week acclimatization in custom-designed metabolic cages, mice underwent CAL (WT + MI, $n = 48$; KO + MI, $n = 45$) or sham surgery (WT + Sham, KO + Sham, $n = 15$) and were maintained thereafter in metabolic cages with free access to food, tap water and water containing 1.8% NaCl. This helped us to compare the intake of normal water versus the salt solution between WT and KO mice, as post-MI mice tend to drink the salt solution more than the tap water provided. Water and salt intake in the form of the 1.8% NaCl solution were measured and 24 h-urine collections were obtained for the duration of the study to demonstrate the effects of TNF on the RAS in CHF [22].

At the end of the study, mice from both protocols were euthanized, blood samples were collected for plasma NE measurement and the hypothalamus and brainstem tissue samples were collected for gene expression, electron spin resonance spectroscopy (ESR) and immunofluorescence studies.

Echocardiography

Echocardiography was performed in mice anesthetized with 1.5% isoflurane in oxygen at 24 h and 4 weeks following CAL/sham surgery to assess cardiac function with a Toshiba Aplio SSH770 system (Toshiba Medical Systems, CA) fitted with a PLT 1202 linear transducer (12 MHz). LV end-diastolic and end-systolic diameter (LVD and LVS, respectively), LV end-diastolic and end-systolic posterior wall thicknesses (PWD and PWS, respectively), and LV percent fractional shortening (%FS) were measured using M-mode imaging. The portion

of the LV that displayed akinesis in 2D short-axis imaging was electronically planimetered and expressed as a percent of the total LV silhouette to estimate the infarct size as previously validated and described [12, 19, 37]. Only mice with infarct sizes of 40–50% were used in the study.

ESR studies

Superoxide and peroxynitrite production in the hypothalamus and brainstem were measured using spin-traps and a BenchTop ESR-spectrophotometer e-scan (Noxygen Science Transfer & Diagnostics GmbH, Elzach, Germany), as previously described [9]. The intensity of ESR spectra was quantified after subtraction of the ESR probe signal without tissue sample.

Semi-quantitative real-time RT-PCR

RNA was isolated from hypothalamus and brainstem tissues with TRIzol (Invitrogen, CA, USA), treated with DNAase, and reverse transcribed using random primers (Supplementary Table 1) and reverse transcriptase. Gene transcripts were determined by quantitative real-time PCR using SYBR-Green master mix (Applied Biosystems, CA, USA) on an Applied Biosystems 7900 system. Gene expression levels were calculated using the $2^{-\Delta\Delta Ct}$ method and normalized to the 18S gene. The data were expressed relative to respective MI + VEH values which were arbitrarily set at 1.

Double-labeling immunofluorescence

Immunofluorescence was performed as previously described [23] with minor modifications. Formalin-fixed sections were labeled by the sequential application of the primary rat anti-rabbit NeuN (Santa Cruz), a primary rat anti-mouse nNOS, or anti-mouse 3-NT, and corresponding biotin-labeled secondary immunoglobulin (IgG) followed by a streptavidin color conjugate complex, Alexafluor 488 or 596 (Molecular Probes). The slides were washed and mounted with ProLong Gold anti-fade reagent (Molecular Probes) for fluorescence microscopy.

Measurement of plasma norepinephrine levels by HPLC

Plasma NE levels were measured using high performance liquid chromatography (HPLC) as described previously [16]. Plasma samples were prepared by adding activated alumina, Tris buffer, EDTA, internal standard DHBA, and 0.5 ml of mouse plasma. The samples were centrifuged and the supernatant separated and rinsed twice in ultra-pure water and filtered through a Millipore filter (Ultrafree MC UFC30GV00, MilliporeCorp). Samples were injected into an Eicom HTEC-500 system fitted with a HPLC-electrochemical detector.

Data analyses

All data illustrated are expressed as mean ± SEM. Statistical analyses were performed using GraphPad Prism v5.00 (GraphPad Software, CA, http://www.graphpad.com). Log-rank (Mantel-Cox) test was used to compare the survival rates between groups. Student's *t* test or one-way ANOVA was used to observe the differences among groups, and two-way or repeated measures ANOVA was used for comparison of metabolic parameters, followed by Bonferroni's correction. Spearman's correlation was used to measure the strength of the relationship between 24 h sodium excretion and calculated daily sodium intake. In all cases, $p < 0.05$ was considered significant.

Results

Improved survival in KO and ETN-treated mice post-MI

In protocol I, 27.3% mortality was observed in MI + VEH mice, while the mortality rate was reduced to 10% in MI + ETN mice (Fig. 1a). In protocol II, <5% mortality was observed in both KO and WT + Sham mice, while the mortality was 20.1% in WT + MI and 6.7% in KO + MI mice. Most deaths occurred by day-10 and were a result of cardiac rupture as determined by autopsy. However, compared to the Sham mice, significantly more WT + MI mice ($p = 0.0054$) died during the study than the KO + MI mice ($p = 0.15$) (Fig. 1b). This suggests that TNF inhibition might improve long-term survival post-MI.

TNF is involved in fluid and sodium retention in CHF

Figure 2 shows the effect of TNF on fluid intake, urine output (UO), sodium intake and urinary sodium excretion (U_{Na}) in WT and KO mice. Water intake decreased significantly, while sodium intake dramatically increased by days 2–3 in WT + MI mice. However, after day-3, and through the conclusion of the study, water intake remained constant in all experimental groups, while sodium intake remained elevated in WT + MI mice, but not in the Sham or KO + MI mice. UO and U_{Na} decreased significantly in WT + MI mice. Conversely, UO and U_{Na} in the KO + MI mice decreased until day 3, but later returned to levels similar to Sham mice. In this study, dietary sodium intake from solid food and fecal sodium excretion were not considered, as there was no significant difference in food intake solid food between the groups.

In sham-operated WT and KO mice, the correlation coefficients between daily sodium intake and U_{Na} excretion were 0.26 ($p = 0.24$) and −0.24 ($p = 0.27$), respectively. However, a negative correlation of −0.82 ($p < 0.0001$) was observed between sodium-intake and U_{Na} in WT + MI while the corresponding correlation coefficient was positive 0.66 ($p < 0.01$) in KO + MI mice, suggesting that adverse salt and fluid retention in CHF mice is partly mediated by TNF.

Central TNF inhibition reduces cardiac dysfunction post-MI

Echocardiography revealed a decline in %FS associated with increases in systolic LV chamber dimensions and wall thicknesses after 4 weeks in MI + VEH mice, but not in MI + ETN mice (Table 1). Similar findings were observed at 4 weeks in WT + MI versus KO + MI mice (Table 1), indicating that TNF contributes to deteriorating cardiac function and structure following CAL.

Heart and lung weight to body weight (HW/BW and LW/BW, respectively) ratios were measured after the 4-week study as indices of cardiac remodeling and pulmonary congestion (Table 1), respectively. Compared to the WT + Sham mice, the wet LW/BW ratios were significantly higher in the WT + MI mice, suggesting the development of fluid retention (as correlated by Fig. 2 results) and pulmonary congestion. However, no significant differences among the HW/BW ratios were observed. Nevertheless, LW/BW ratios in MI + ETN and KO + MI mice were significantly lower than those in WT + MI mice, demonstrating decreased pulmonary congestion with TNF ablation.

TNF blockade decreases PIC expression in the hypothalamus and brainstem in CHF

The transcript levels of TNF and IL-1β were higher in the hypothalamus and brainstem of MI + VEH as compared to MI + ETN and KO + MI mice, indicating that TNF blockade results in the decreased expression of PICs, including TNF, in these cardio-regulatory centers. IL-6 expression was unchanged. Conversely, in MI + VEH mice, the decreased IL-10 expression, an anti-inflammatory cytokine, was restored in MI + ETN and KO + MI

mice (Table 2), underscoring the role that TNF inhibition has on normalizing the PIC balance and improving the anti-inflammatory actions in post-MI mice. Caution, however, must be used when reviewing these results, as the vehicle used for MI + VEH was simply aCSF without the IgG antibody typically used as the ETN control.

TNF alters expression of $O_2^{\cdot-}$ and NO in the hypothalamus and brainstem in CHF

The expression of Nox2, the major catalytic subunit of NADPH oxidase, was up-regulated in the PVN of MI + VEH as compared to MI + ETN mice. These levels were also higher in WT + MI mice compared to the KO + MI mice (Table 2). Nox4 was unchanged. These findings are consistent with the $O_2^{\cdot-}$ production observed in the PVN by ESR (Fig. 3). Though $O_2^{\cdot-}$ was increased in the VLM, Nox2 expression was not, indicating a possible alternate mechanism and source. However, TNF ablation reduced $O_2^{\cdot-}$ production, indicating a role for TNF in ROS activation.

Neuronal NOS (nNOS) expression significantly decreased in the hypothalamus and brainstem, while that of inducible NOS (iNOS) was increased in the hypothalami of MI + VEH and WT + MI mice versus Sham mice. ETN-treatment and TNF gene deletion prevented these changes (Table 2).

Immunofluorescence studies demonstrated a significant decrease in the number of nNOS-positive neurons in the VLM of WT + MI mice versus the Sham groups. Neurons were identified by co-staining with the neuronal marker NeuN. The number of nNOS-positive neurons in the VLM of KO + MI mice was unchanged from that of TNF + Sham mice (Fig. 4). We observed a similar pattern of nNOS expression in the PVN (Data not shown).

TNF plays a role in the interaction between $O_2^{\cdot-}$ and NO in CHF

We confirmed the formation of OONO· in the PVN and VLM by ESR (Fig. 3). CHF resulted in increased OONO· levels in these brain regions in MI + VEH mice versus MI + ETN mice. In addition, higher OONO· production was observed in WT + MI as compared to KO + MI mice. Although $O_2^{\cdot-}$ and OONO· are produced in other brain regions, only the PVN and VLM showed significant differences in CHF and Sham mice. Therefore, quantitative analyses presented are focused only on these regions.

To further assess the interaction between $O_2^{\cdot-}$ and NO in the PVN and VLM regions, we used immunofluorescence co-staining of nNOS and 3-NT, a product of OONO·. The percent of nNOS-positive cells that stained for 3-NT were comparatively higher in the PVN 4-week post-MI in both WT and KO mice versus their respective Sham groups. However, the number of 3-NT-positive neurons was significantly higher in WT + MI as compared to KO + MI mice (Fig. 5). Similar effects with regard to nNOS and 3-NT expression were seen in the VLM region of WT and KO mice with/without CHF (data not shown). These results show the involvement of TNF in adversely altering NO and $O_2^{\cdot-}$ production, while also increasing their interaction and the deleterious production of OONO· in CHF.

TNF alters angiotensin receptor expression in the hypothalamus and brainstem in CHF

We observed an increase in AT1R expression in the hypothalamus and brainstem of MI + VEH versus MI + ETN mice (Table 2). Similar increases in the AT1R expression in these regions was observed in WT + MI over KO + MI mice (Table 2). Conversely, CHF was associated with a decrease in AT2R expression in these brain regions in WT as compared to KO and ETN-treated mice (Table 2). No difference was observed in the expression of these receptors in Sham mice, signifying the cross-talk existent between TNF and RAS components in the progression of CHF.

Central TNF mediates neuronal activation and sympathoexcitation in CHF

Chronic neuronal activation in the PVN and VLM was studied using an antibody that detects all members of the Fos family; c-Fos, FosB, Fra1 and Fra2. CHF induced a markedly greater number of Fos-positive neurons in WT as compared to the KO and ETN-treated mice (Fig. 6a). It should be noted that in Sham mice, the number of Fos-positive neurons were unchanged (Fig. 6b).

Plasma NE levels, an indirect indicator for sympathoexcitation, were elevated in MI + VEH andWT + MI mice (Fig. 6c). This increase, however, was attenuated in MI + ETN, Sham and KO + MI mice, suggesting the role of TNF in neuronal activation and sympathoexcitation in CHF.

Discussion

The present study highlights several important findings: (1) increased sodium and fluid retention observed in CHF are partly dependent upon elevated PICs; (2) central TNF blockade reduces NADPH oxidase subunit and PIC expression and ROS production, and decreases sympathoexcitation in the cardiovascular regulatory regions of the brain; (3) central TNF blockade and/or TNF gene deletion prevents the CHF-induced reduction nNOS in the PVN and VLM; and (4) blocking TNF reduces OONO· formation and reduces neuronal excitation in CHF. These findings support our hypothesis that the resultant sympathetic hyperactivity in CHF is due, in part, to TNF-induced oxidative stress and AT1Rs in the sympathoexcitatory neurons of the PVN and VLM.

Our previous studies demonstrated that systemic administration of anti-cytokine agents can lower brain PIC synthesis, NADPH oxidase subunit expression and superoxide production in CHF [16]. This is further supported by findings from the current study using KO mice and mice with TNF centrally inhibited. Additionally, the present study demonstrates that central cytokine inhibition reduces ROS production in the PVN and VLM regions, resulting in reduced neurohumoral excitation. This strongly indicates that central TNF levels are intrinsically involved in the NADPH oxidase activation, ROS production and sympathoexcitation seen in CHF. Increased $O_2^{\cdot-}$ production in the RVLM, induced by subchronic ICV AngII infusion, is associated with elevated basal SNA and impaired arterial baroreflex function [14]. Moreover, bilateral microinjections of the ROS scavengers tempol or tiron into the RVLM attenuated the pressor, sympathetic, and tachycardic responses to central AngII microinjection [32]. Interestingly, the $O_2^{\cdot-}$ source in both cases appears to be NADPH oxidase. In this study, the elevated expression levels of the catalytic subunits of NADPH oxidase, Nox2 and Nox4, in CHF, were significantly attenuated in the hypothalamus of mice treated ICV with ETN as well as in conventional TNF KO mice. The attenuated $O_2^{\cdot-}$ levels in the PVN and VLM with ETN treatment clearly delineate a role for TNF in CHF-induced ROS production.

The abnormal drinking behavior and salt intake in response to AngII infusion was shown to be mediated via NADPH oxidase-induced $O_2^{\cdot-}$ production [52, 53]. Indeed, most of the effects of the RAS, including fluid balance and endocrine secretion, are mediated by AT1Rs [43]. Our metabolic studies also show that in WT + MI mice, there is a significant negative correlation ($r = -0.82$) between sodium intake and U_{Na}, indicating a more profound increase in sodium and water retention versus Sham mice. Conversely, we found a significant positive correlation between sodium intake and U_{Na} ($r = 0.66$) in KO + MI mice, indicating the role of TNF in fluid and sodium retention in CHF. These changes were associated with an increased AT1R and a decreased AT2R expression within the hypothalamus and brainstem, as previously described [12]. Moreover, increased fluid retention and pulmonary

congestion in WT + MI versus KO + MI mice indicate that TNF-induced elevation in $O_2^{\cdot-}$ and AT1Rs in the PVN and VLM might be contributing to the unusual drinking behavior and sodium and fluid retention in CHF.

High levels of AngII in the CNS can enhance sympathoexcitation through AT1R activation [28, 36, 45] and downregulation of nNOS, the primary source of NO in CNS neurons [3]. NO, a well known sympatho-inhibitory neurotransmitter in the CNS, following ICV inhibition, results in elevated arterial pressure and sympathetic outflow [35, 49]. Conversely, blockade of AT1Rs with a concomitant infusion of a NO donor in CHF lowers the basal SNA, suggesting an important correlation between AngII and NO [30, 55]. Besides AngII, elevated TNF levels in the PVN can also evoke sympathoexcitation [16]. TNF blockade in this study attenuated NE levels and AT1R expression in the hypothalamus and brainstem, suggesting a major intermediary role for TNF in neurohumoral excitation. Furthermore, increased nNOS in the PVN and VLM by TNF blockade indicates a role for TNF in altering NO-induced sympatho-inhibitory effects.

Administration of AngII ICV decreases nNOS, with a concurrent increase in ROS, in the PVN, ultimately leading to increased sympathoexcitation [4]. Our previous study using pentoxifylline, a cytokine inhibitor, in CHF rats, increased the attenuated nNOS in the PVN [17]. In the current study, ICV inhibition of TNF antagonized the NO-depleting effects and sympathoexcitation seen in CHF. Moreover, following MI, elevation of TNF has been observed even before that of many neurohormones, including AngII [41]. Therefore, it is possible that the increased TNF observed following MI can trigger the production of other peptides and mediators that lead to neurohumoral excitation.

CHF induced an increase in iNOS expression in the PVN and RVLM with a concurrent increase in $O_2^{\cdot-}$, resulting in additional formation of OONO· in these regions of WT + MI mice, thereby negating NO's sympatho-inhibitory effects. Zanzinger et al. [48] previously reported that $O_2^{\cdot-}$ and NO interact in the RVLM, resulting in the formation of OONO· that caused neuronal damage. They later demonstrated that microinjection of OONO· into the RVLM caused dose-dependent transient excitatory responses [47]. The present study's results indicate that in CHF, TNF contributes significantly to the interaction of $O_2^{\cdot-}$ and NO in the PVN and RVLM. It is also possible that the $O_2^{\cdot-}$ and NO produced from eNOS and iNOS in other cells, as well as from other regions of the brain, diffuse into the neurons of the PVN and VLM and contribute towards increased neuronal formation of OONO·. Also, elevated iNOS, when uncoupled, can produce more $O_2^{\cdot-}$ and augment NO depletion. The reduced nNOS and increased ROS produced in the PVN and RVLM decreases the bioavailability of NO [48], thereby contributing to sympathoexcitation.

ROS act as key modulators of increased neuronal activity in the PVN and supraoptic nucleus (SON) of CHF animals [29, 46]. The expression of FosB, Fra1, and Fra2 remains elevated under conditions of chronic neuronal stimulation, such as CHF [44]. Here, CHF-induced Fos expression in the PVN and RVLM was attenuated by TNF blockade, suggesting a role for TNF in neuronal excitation in CHF. These results were comparable to previous studies where increased Fos-positive neurons were detected in the PVN and SON at both 2- and 4-week post-MI [29]. Additionally, elevated AngII levels in CHF can induce Fos activation in the PVN and SON, which can be inhibited by a ROS scavenger, indicating the importance of AngII-induced ROS in sympathoexcitation [29]. Also, the c-Jun/JNK/c-Fos pathway is involved in the up-regulation of AT1R expression by specific transcription factors [6]. All these changes, indeed, were associated with improved cardiac function. Taken together, results from the present study raise the intriguing possibility that TNF induces Fos

expression via modulation of ROS in the PVN and RVLM through an AT1R mediated mechanism.

In conclusion, this study suggests a biologically important cross-talk between the RAS and PICs in the PVN and VLM in CHF. Functionally, this cross-talk leads to uncontrolled production of ROS, which can in turn act as second messengers for further amplification of TNF and/or AngII activation, resulting in increased neuronal firing in the PVN and RVLM, contributing to sodium/fluid imbalances, and exacerbating sympathoexcitation and disease progression in the failing heart (Fig. 7). Future studies will explore the molecular mechanisms by which central TNF signals the downstream sympathoexcitatory circuits.

Perspectives

Increased sympathetic outflow is a major prognostic determinant in CHF patients. Interventions aimed at reducing sympathetic drive are, therefore, of major clinical interest. Presently, we show that in ETN-treated and TNF KO mice, CHF-induced ROS production is attenuated and NO levels are restored in the PVN and VLM, thereby reducing sympathoexcitation. Although previous clinical reports indicated that the results of anti-cytokine therapies in CHF patients were uncertain, confounding factors may have affected the outcome, including additional patient drug therapies received during the experimental trials and the use of non-tissue target specific whole body drug administration techniques [10, 24, 31, 41]. Furthermore, our results suggest that in addition to its direct toxic effects exerted on the heart and circulation [5, 8, 25, 40, 50, 54], TNF also contributes significantly to a central oxidative imbalance, resulting in uncontrolled sympathoexcitation and causing the progression of CHF. In the future, it will be of interest to determine whether inclusion of an anti-cytokine agent that crosses the BBB in the treatment regimen of CHF patients may change clinical outcomes.

Supplementary Material

Refer to Web version on PubMed Central for supplementary material.

Acknowledgments

This work was supported by National Heart, Lung, and Blood Institute Grant (1RO1 HL-080544-01 to J.F.). The authors acknowledge the expert technical assistance of Elizabeth McIlwain, Philip J. Ebenezer, Michael Broussard and Sherry Ring.

References

1. Banks WA. Blood–brain barrier transport of cytokines: a mechanism for neuropathology. Curr Pharm Des. 2005; 11:973–984. [PubMed: 15777248]
2. Bozkurt B, Kribbs SB, Clubb FJ Jr, Michael LH, Didenko VV, Hornsby PJ, Seta Y, Oral H, Spinale FG, Mann DL. Pathophysiologically relevant concentrations of tumor necrosis factor-alpha promote progressive left ventricular dysfunction and remodeling in rats. Circulation. 1998; 97:1382–1391. [PubMed: 9577950]
3. Campese VM, Shaohua Y, Huiquin Z. Oxidative stress mediates angiotensin II-dependent stimulation of sympathetic nerve activity. Hypertension. 2005; 46:533–539. [PubMed: 16116043]
4. Campese VM, Ye S, Zhong H. Downregulation of neuronal nitric oxide synthase and interleukin-1beta mediates angiotensin II-dependent stimulation of sympathetic nerve activity. Hypertension. 2002; 39:519–524. [PubMed: 11882601]
5. Canton M, Skyschally A, Menabo R, Boengler K, Gres P, Schulz R, Haude M, Erbel R, Di Lisa F, Heusch G. Oxidative modification of tropomyosin and myocardial dysfunction following coronary microembolization. Eur Heart J. 2006; 27:875–881. [PubMed: 16434410]

6. Chan JY, Wang LL, Lee HY, Chan SH. Augmented upregulation by c-fos of angiotensin subtype 1 receptor in nucleus tractus solitarii of spontaneously hypertensive rats. Hypertension. 2002; 40:335–341. [PubMed: 12215476]
7. Chappell D, Hofmann-Kiefer K, Jacob M, Rehm M, Briegel J, Welsch U, Conzen P, Becker BF. TNF-alpha induced shedding of the endothelial glycocalyx is prevented by hydrocortisone and antithrombin. Basic Res Cardiol. 2009; 104:78–89. [PubMed: 18836678]
8. Chorianopoulos E, Heger T, Lutz M, Frank D, Bea F, Katus HA, Frey N. FGF-inducible 14 kDa protein (Fn14) is regulated via the RhoA/ROCK kinase pathway in cardiomyocytes and mediates nuclear factor-kappaB activation by TWEAK. Basic Res Cardiol. 2010; 105:301–313. [PubMed: 19629561]
9. Dikalov SI, Dikalova AE, Mason RP. Noninvasive diagnostic tool for inflammation-induced oxidative stress using electron spin resonance spectroscopy and an extracellular cyclic hydroxylamine. Arch Biochem Biophys. 2002; 402:218–226. [PubMed: 12051666]
10. Fildes JE, Shaw SM, Yonan N, Williams SG. The immune system and chronic heart failure: is the heart in control? J Am Coll Cardiol. 2009; 53:1013–1020. S0735-1097(09)00024-2 [pii]. [PubMed: 19298913]
11. Fleegal-DeMotta MA, Doghu S, Banks WA. Angiotensin II modulates BBB permeability via activation of the AT(1) receptor in brain endothelial cells. J Cereb Blood Flow Metab. 2009; 29:640–647. [PubMed: 19127280]
12. Francis J, Weiss RM, Wei SG, Johnson AK, Felder RB. Progression of heart failure after myocardial infarction in the rat. Am J Physiol Regul Integr Comp Physiol. 2001; 281:R1734–R1745. [PubMed: 11641147]
13. Galiano M, Liu ZQ, Kalla R, Bohatschek M, Koppius A, Gschwendtner A, Xu S, Werner A, Kloss CU, Jones LL, Bluethmann H, Raivich G. Interleukin-6 (IL6) and cellular response to facial nerve injury: effects on lymphocyte recruitment, early microglial activation and axonal outgrowth in IL6-deficient mice. Eur J Neurosci. 2001; 14:327–341. ejn1647 [pii]. [PubMed: 11553283]
14. Gao L, Wang W, Li YL, Schultz HD, Liu D, Cornish KG, Zucker IH. Sympathoexcitation by central ANG II: roles for AT1 receptor upregulation and NAD(P)H oxidase in RVLM. Am J Physiol Heart Circ Physiol. 2005; 288:H2271–H2279. 00949.2004 [pii]. [PubMed: 15637113]
15. Gloor SM, Wachtel M, Bolliger MF, Ishihara H, Landmann R, Frei K. Molecular and cellular permeability control at the blood-brain barrier. Brain Res Brain Res Rev. 2001; 36:258–264. S0165017301001023 [pii]. [PubMed: 11690623]
16. Guggilam A, Haque M, Kerut EK, McIlwain E, Lucchesi P, Seghal I, Francis J. TNF-alpha blockade decreases oxidative stress in the paraventricular nucleus and attenuates sympathoexcitation in heart failure rats. Am J Physiol Heart Circ Physiol. 2007; 293:H599–H609. 00286.2007 [pii]. [PubMed: 17416605]
17. Guggilam A, Patel KP, Haque M, Ebenezer PJ, Kapusta DR, Francis J. Cytokine blockade attenuates sympathoexcitation in heart failure: cross-talk between nNOS, AT-1R and cytokines in the hypothalamic paraventricular nucleus. Eur J Heart Fail. 2008; 10:625–634. S1388-9842(08)00196-7 [pii]. [PubMed: 18550427]
18. Han Y, Shi Z, Zhang F, Yu Y, Zhong MK, Gao XY, Wang W, Zhu GQ. Reactive oxygen species in the paraventricular nucleus mediate the cardiac sympathetic afferent reflex in chronic heart failure rats. Eur J Heart Fail. 2007; 9:967–973. S1388-9842(07)00267-X [pii]. [PubMed: 17719272]
19. Hill JA, Karimi M, Kutschke W, Davisson RL, Zimmerman K, Wang Z, Kerber RE, Weiss RM. Cardiac hypertrophy is not a required compensatory response to short-term pressure overload. Circulation. 2000; 101:2863–2869. [PubMed: 10859294]
20. Hu K, Bahner U, Gaudron P, Palkovits M, Ring M, Fehle A, Kruse B, Ertl G. Chronic effects of ACE-inhibition (quinapril) and angiotensin-II-type-1 receptor blockade (losartan) on atrial natriuretic peptide in brain nuclei of rats with experimental myocardial infarction. Basic Res Cardiol. 2001; 96:258–266. [PubMed: 11403419]
21. Huang CH, Vallejo JG, Kollias G, Mann DL. Role of the innate immune system in acute viral myocarditis. Basic Res Cardiol. 2009; 104:228–237. [PubMed: 19159057]

22. Johnson AK, Thunhorst RL. The neuroendocrinology of thirst and salt appetite: visceral sensory signals and mechanisms of central integration. Front Neuroendocrinol. 1997; 18:292–353. S0091-3022(97)90153-9 [pii]. [PubMed: 9237080]
23. Khaleduzzaman M, Francis J, Corbin ME, McIlwain E, Boudreaux M, Du M, Morgan TW, Peterson KE. Infection of cardiomyocytes and induction of left ventricle dysfunction by neurovirulent polytropic murine retrovirus. J Virol. 2007; 81:12307–12315. JVI.01002-07 [pii]. [PubMed: 17855522]
24. Kleinbongard P, Heusch G, Schulz R. TNF alpha in atherosclerosis, myocardial ischemia/reperfusion and heart failure. Pharmacol Ther. 2010; 127:295–314. S0163-7258(10)00114-2 [pii]. [PubMed: 20621692]
25. Krown KA, Page MT, Nguyen C, Zechner D, Gutierrez V, Comstock KL, Glembotski CC, Quintana PJ, Sabbadini RA. Tumor necrosis factor alpha-induced apoptosis in cardiac myocytes. Involvement of the sphingolipid signaling cascade in cardiac cell death. J Clin Invest. 1996; 98:2854–2865. [PubMed: 8981934]
26. Lacerda L, McCarthy J, Mungly SF, Lynn EG, Sack MN, Opie LH, Lecour S. TNFalpha protects cardiac mitochondria independently of its cell surface receptors. Basic Res Cardiol. 2010; 105:751–762. [PubMed: 20680307]
27. Li S, Zhong S, Zeng K, Luo Y, Zhang F, Sun X, Chen L. Blockade of NF-kappaB by pyrrolidine dithiocarbamate attenuates myocardial inflammatory response and ventricular dysfunction following coronary microembolization induced by homologous microthrombi in rats. Basic Res Cardiol. 2010; 105:139–150. [PubMed: 19823892]
28. Li YF, Wang W, Mayhan WG, Patel KP. Angiotensin-mediated increase in renal sympathetic nerve discharge within the PVN: role of nitric oxide. Am J Physiol Regul Integr Comp Physiol. 2006; 290:R1035–R1043. 00338.2004 [pii]. [PubMed: 16322353]
29. Lindley TE, Doobay MF, Sharma RV, Davisson RL. Superoxide is involved in the central nervous system activation and sympathoexcitation of myocardial infarction-induced heart failure. Circ Res. 2004; 94:402–409. [PubMed: 14684626]
30. Liu JL, Zucker IH. Regulation of sympathetic nerve activity in heart failure: a role for nitric oxide and angiotensin II. Circ Res. 1999; 84:417–423. [PubMed: 10066676]
31. Mann DL, McMurray JJ, Packer M, Swedberg K, Borer JS, Colucci WS, Djian J, Drexler H, Feldman A, Kober L, Krum H, Liu P, Nieminen M, Tavazzi L, van Veldhuisen DJ, Waldenstrom A, Warren M, Westheim A, Zannad F, Fleming T. Targeted anticytokine therapy in patients with chronic heart failure: results of the Randomized Etanercept Worldwide Evaluation (RENEWAL). Circulation. 2004; 109:1594–1602. [PubMed: 15023878]
32. Mayorov DN, Head GA, De Matteo R. Tempol attenuates excitatory actions of angiotensin II in the rostral ventrolateral medulla during emotional stress. Hypertension. 2004; 44:101–106. [PubMed: 15159379]
33. McCann SM, Kimura M, Karanth S, Yu WH, Mastronardi CA, Rettori V. The mechanism of action of cytokines to control the release of hypothalamic and pituitary hormones in infection. Ann N Y Acad Sci. 2000; 917:4–18. [PubMed: 11268367]
34. Raivich G, Moreno-Flores MT, Muller JC, Kreutzberg GW. Regulation of microglial proliferation: colony-stimulating factors and their receptors. Neuropathol Appl Neurobiol. 1994; 20:209–211. [PubMed: 8072668]
35. Sakuma I, Togashi H, Yoshioka M, Saito H, Yanagida M, Tamura M, Kobayashi T, Yasuda H, Gross SS, Levi R. NG-methyl-l-arginine, an inhibitor of l-arginine-derived nitric oxide synthesis, stimulates renal sympathetic nerve activity in vivo. A role for nitric oxide in the central regulation of sympathetic tone? Circ Res. 1992; 70:607–611. [PubMed: 1537096]
36. Sasaki S, Dampney RA. Tonic cardiovascular effects of angiotensin II in the ventrolateral medulla. Hypertension. 1990; 15:274–283. [PubMed: 2303285]
37. Schiller NB, Acquatella H, Ports TA, Drew D, Goerke J, Ringertz H, Silverman NH, Brundage B, Botvinick EH, Boswell R, Carlsson E, Parmley WW. Left ventricular volume from paired biplane two-dimensional echocardiography. Circulation. 1979; 60:547–555. [PubMed: 455617]

38. Sheng JG, Mrak RE, Griffin WS. Enlarged and phagocytic, but not primed, interleukin-1 alpha-immunoreactive microglia increase with age in normal human brain. Acta Neuropathol. 1998; 95:229–234. [PubMed: 9542587]
39. Shi P, Diez-Freire C, Jun JY, Qi Y, Katovich MJ, Li Q, Sriramula S, Francis J, Sumners C, Raizada MK. Brain microglial cytokines in neurogenic hypertension. Hypertension. 56:297–303. HYPERTENSIONAHA.110.150409 [pii]. [PubMed: 20547972]
40. Thielmann M, Dorge H, Martin C, Belosjorow S, Schwanke U, van De Sand A, Konietzka I, Buchert A, Kruger A, Schulz R, Heusch G. Myocardial dysfunction with coronary microembolization: signal transduction through a sequence of nitric oxide, tumor necrosis factor-alpha, and sphingosine. Circ Res. 2002; 90:807–813. [PubMed: 11964374]
41. Torre-Amione G, Kapadia S, Benedict C, Oral H, Young J, Mann D. Proinflammatory cytokine levels in patients with depressed left ventricular ejection fraction: a report from the Studies of Left Ventricular Dysfunction (SOLVD). J Am Coll Cardiol. 1996; 27:1201–1206. [PubMed: 8609343]
42. Tsutamoto T, Hisanaga T, Wada A, Maeda K, Ohnishi M, Fukai D, Mabuchi N, Sawaki M, Kinoshita M. Interleukin-6 spillover in the peripheral circulation increases with the severity of heart failure, and the high plasma level of interleukin-6 is an important prognostic predictor in patients with congestive heart failure. J Am Coll Cardiol. 1998; 31:391–398. [PubMed: 9462584]
43. Unger T, Badoer E, Ganten D, Lang RE, Rettig R. Brain angiotensin: pathways and pharmacology. Circulation. 1988; 77:I40–I54. [PubMed: 2836110]
44. Vahid-Ansari F, Leenen FH. Pattern of neuronal activation in rats with CHF after myocardial infarction. Am J Physiol. 1998; 275:H2140–H2146. [PubMed: 9843814]
45. Veerasingham SJ, Leenen FH. Excitotoxic lesions of the ventral anteroventral third ventricle and pressor responses to central sodium, ouabain and angiotensin II. Brain Res. 1997; 749:157–160. S0006-8993(96)01381-9 [pii]. [PubMed: 9070643]
46. Wei SG, Zhang ZH, Yu Y, Felder RB. Systemically administered tempol reduces neuronal activity in paraventricular nucleus of hypothalamus and rostral ventrolateral medulla in rats. J Hypertens. 2009; 27:543–550. [PubMed: 19330914]
47. Yu Y, Zhang ZH, Wei SG, Serrats J, Weiss RM, Felder RB. Brain perivascular macrophages and the sympathetic response to inflammation in rats after myocardial infarction. Hypertension. 2010; 55:652–659. [PubMed: 20142564]
48. Zanzinger J. Mechanisms of action of nitric oxide in the brain stem: role of oxidative stress. Auton Neurosci. 2002; 98:24–27. S1566-0702(02)00025-5 [pii]. [PubMed: 12144034]
49. Zanzinger J, Czachurski J, Seller H. Inhibition of basal and reflex-mediated sympathetic activity in the RVLM by nitric oxide. Am J Physiol. 1995; 268:R958–R962. [PubMed: 7733407]
50. Zhang C, Wu J, Xu X, Potter BJ, Gao X. Direct relationship between levels of TNF-alpha expression and endothelial dysfunction in reperfusion injury. Basic Res Cardiol. 2010; 105:453–464. [PubMed: 20091314]
51. Zhang M, Mao Y, Ramirez SH, Tuma RF, Chabrashvili T. Angiotensin II induced cerebral microvascular inflammation and increased blood-brain barrier permeability via oxidative stress. Neuroscience. 2010; 171:852–858. S0306-4522(10)01277-7 [pii]. [PubMed: 20870012]
52. Zimmerman MC, Lazartigues E, Lang JA, Sinnayah P, Ahmad IM, Spitz DR, Davisson RL. Superoxide mediates the actions of angiotensin II in the central nervous system. Circ Res. 2002; 91:1038–1045. [PubMed: 12456490]
53. Zimmerman MC, Lazartigues E, Sharma RV, Davisson RL. Hypertension caused by angiotensin II infusion involves increased superoxide production in the central nervous system. Circ Res. 2004; 95:210–216. [PubMed: 15192025]
54. Zucker IH, Pliquett RU. Novel mechanisms of sympathoexcitation in chronic heart failure. Heart Fail Monit. 2002; 3:2–7. [PubMed: 12634882]
55. Zucker IH, Schultz HD, Li YF, Wang Y, Wang W, Patel KP. The origin of sympathetic outflow in heart failure: the roles of angiotensin II and nitric oxide. Prog Biophys Mol Biol. 2004; 84:217–232. [PubMed: 14769437]

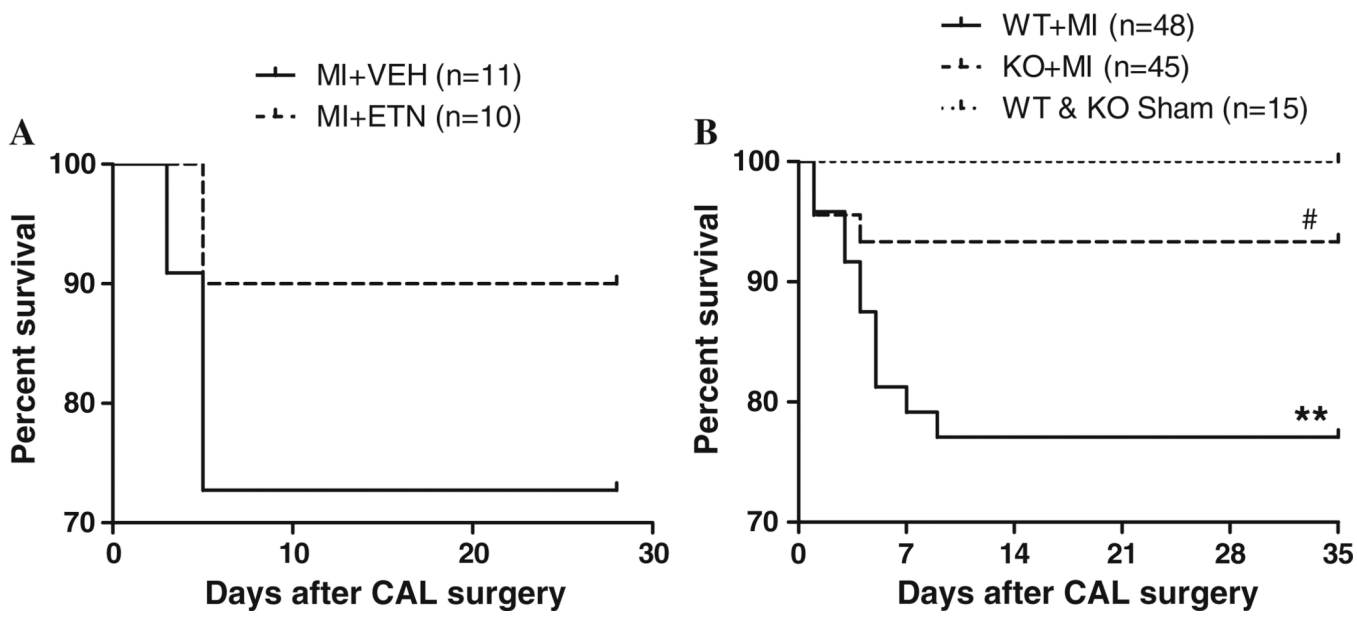

Fig. 1.

Kaplan–Meier survival curves of WT and KO mice at the end of the study. **a** Survival rate was improved in CHF in ETN-treated versus VEH-treated mice. **b** The WT + MI mice exhibited a significant (** $p < 0.01$) decrease in survival compared with sham-operated WT and KO mice 4 weeks post-MI. KO mice demonstrated significantly ($^{\#}$ $p < 0.05$) greater survival when compared with WT 4 weeks post-MI

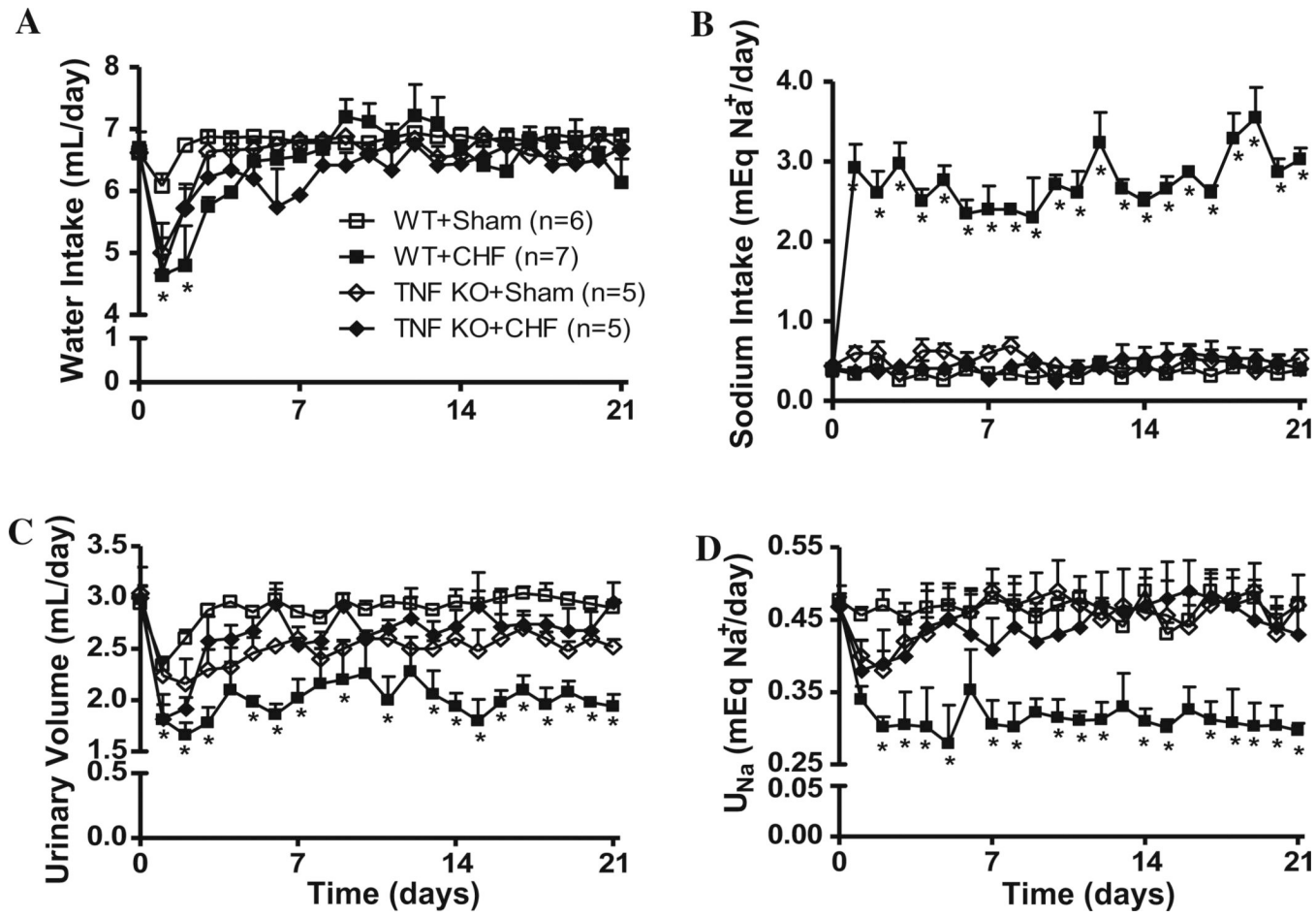

Fig. 2.

Daily water intake (**a**), sodium intake (**b**), urine output (**c**), and sodium excretion (U_{Na}; D) of WT and KO mice during the first 3 weeks post-MI or sham surgery. Data are presented as mean ± SEM

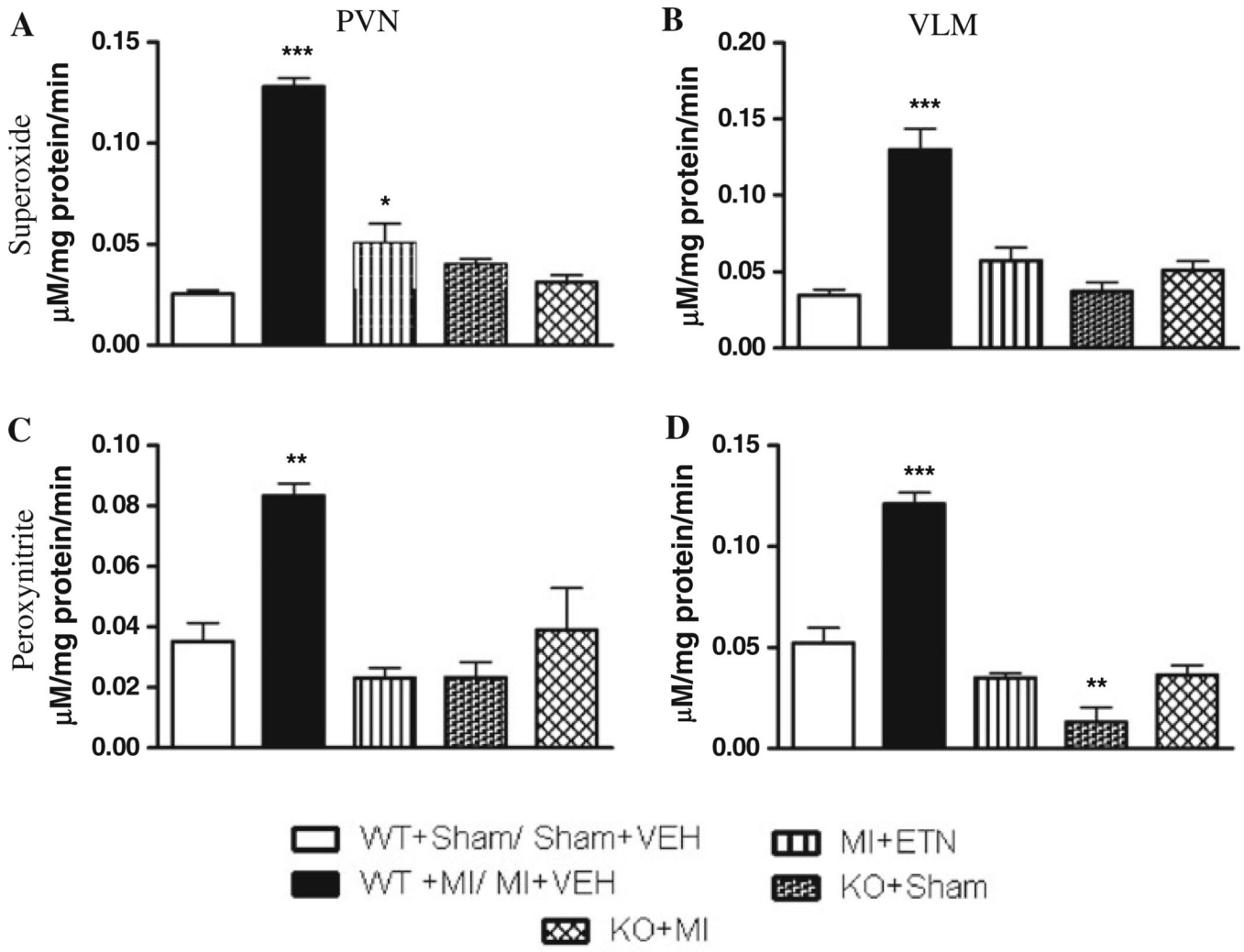

Fig. 3.

a Superoxide anion and **b** peroxynitrite production in the PVN of mice 4 weeks post-MI. **c** Superoxide anion and **d** peroxynitrite production in the VLM of mice 4 weeks post-MI. (* $p < 0.05$, ** $p < 0.01$, *** $p < 0.001$)

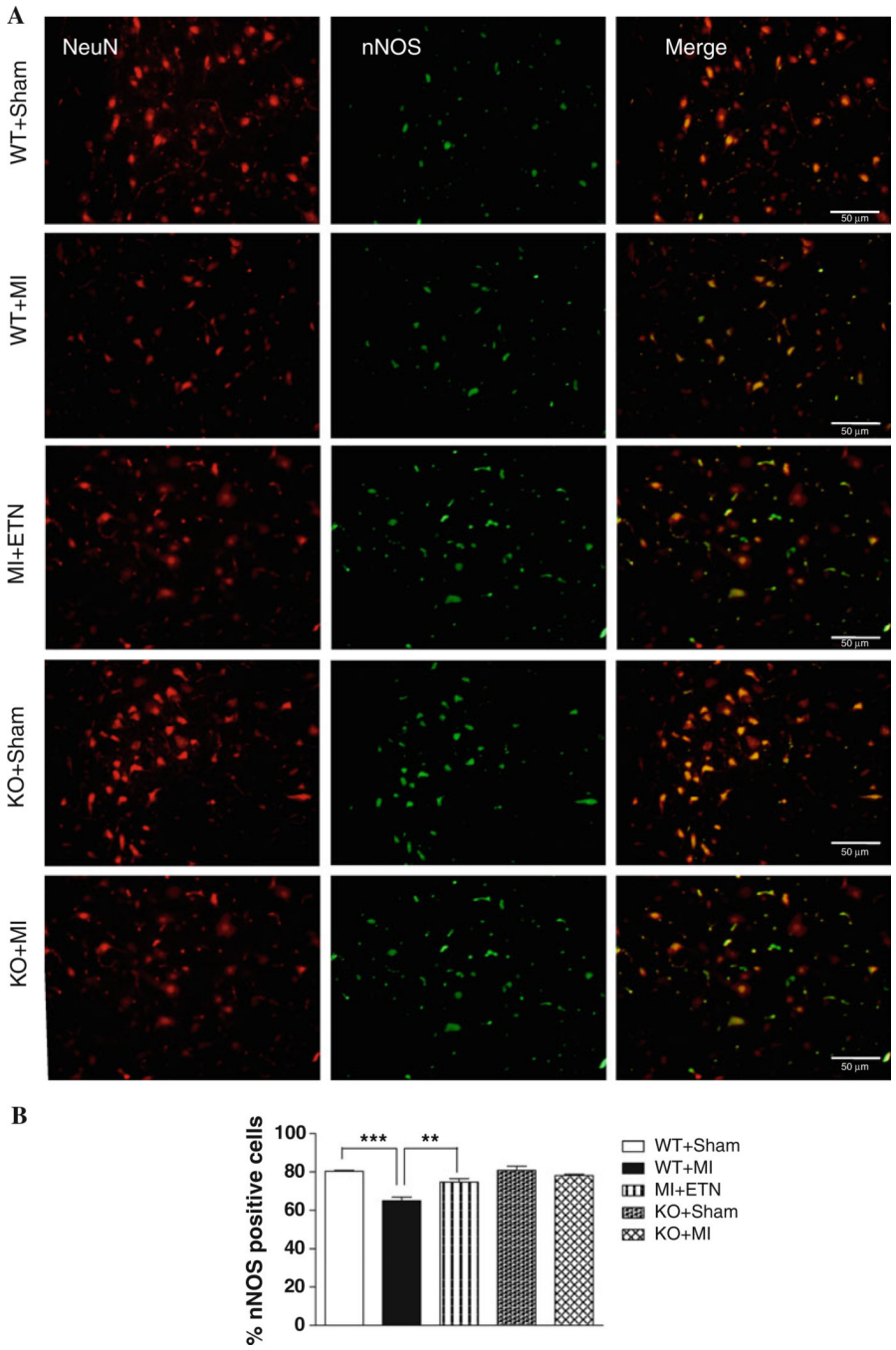

Fig. 4.

a Double-immunofluorescence histochemistry for NeuN, a marker for neuronal nuclei (*left panel*), nNOS (*center panel*), and their overlay (*right panel*) in the VLM. NeuN and nNOS were labeled with AlexaFluor 594 and AlexaFluor 488, respectively. *Scale bar* 50 µm. **b** Total number of $nNOS^+$ cells are lower in WT + MI group (*** $p < 0.001$) when compared with WT + Sham. There is no difference in the $nNOS^+$ neurons in KO mice 4 weeks post-MI

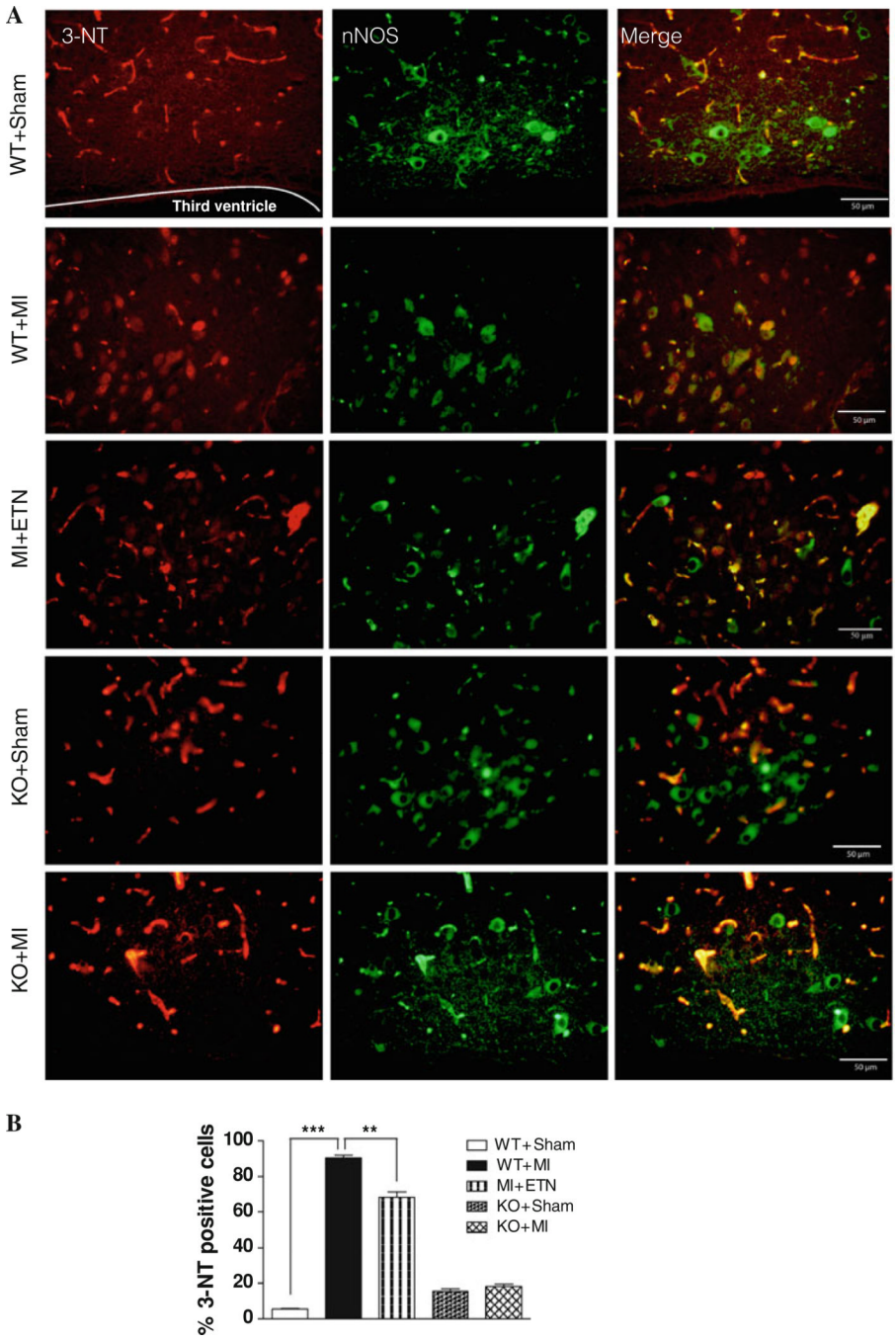

Fig. 5.

a Double-immunofluorescence histochemistry for 3-NT (*left panel*), nNOS (*center panel*), and their overlapping (*right panel*) in the PVN. 3-NT and nNOS were labeled with AlexaFluor 594 and AlexaFluor 488, respectively. *Scale bar* 50 μm. **b** Total number of 3-NT^+ cells are higher in WT + MI group (*** $p < 0.001$) when compared with WT + Sham. There is no difference in the 3-NT positive neurons in KO 4 weeks post-MI when compared with sham mice

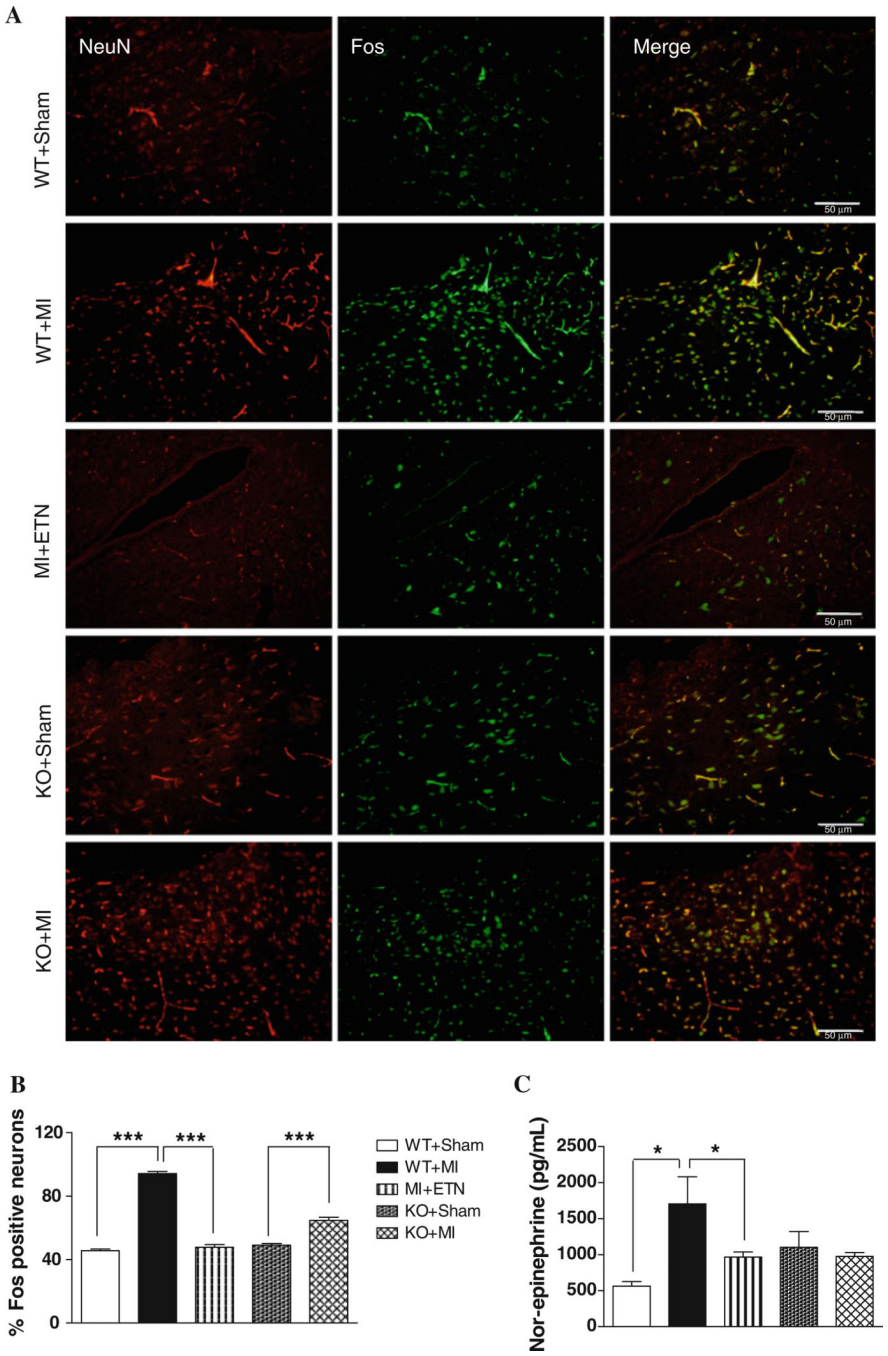

Fig. 6.

a Double-immunofluorescence histochemistry for NeuN (*left panel*), Fos (*center panel*), and their overlapping (*right panel*) in the PVN. NeuN and Fos were labeled with AlexaFluor 594 and AlexaFluor 488, respectively. *Scale bar* 50 μm. **b** Total number of Fos^+ cells are higher in WT + MI group (*** $p < 0.001$) when compared with WT + Sham. There is no difference in the Fos^+ neurons in KO mice 4 weeks post-MI compared to sham mice. **c** Plasma NE levels were significantly higher in WT versus KO mice 4 weeks post-MI

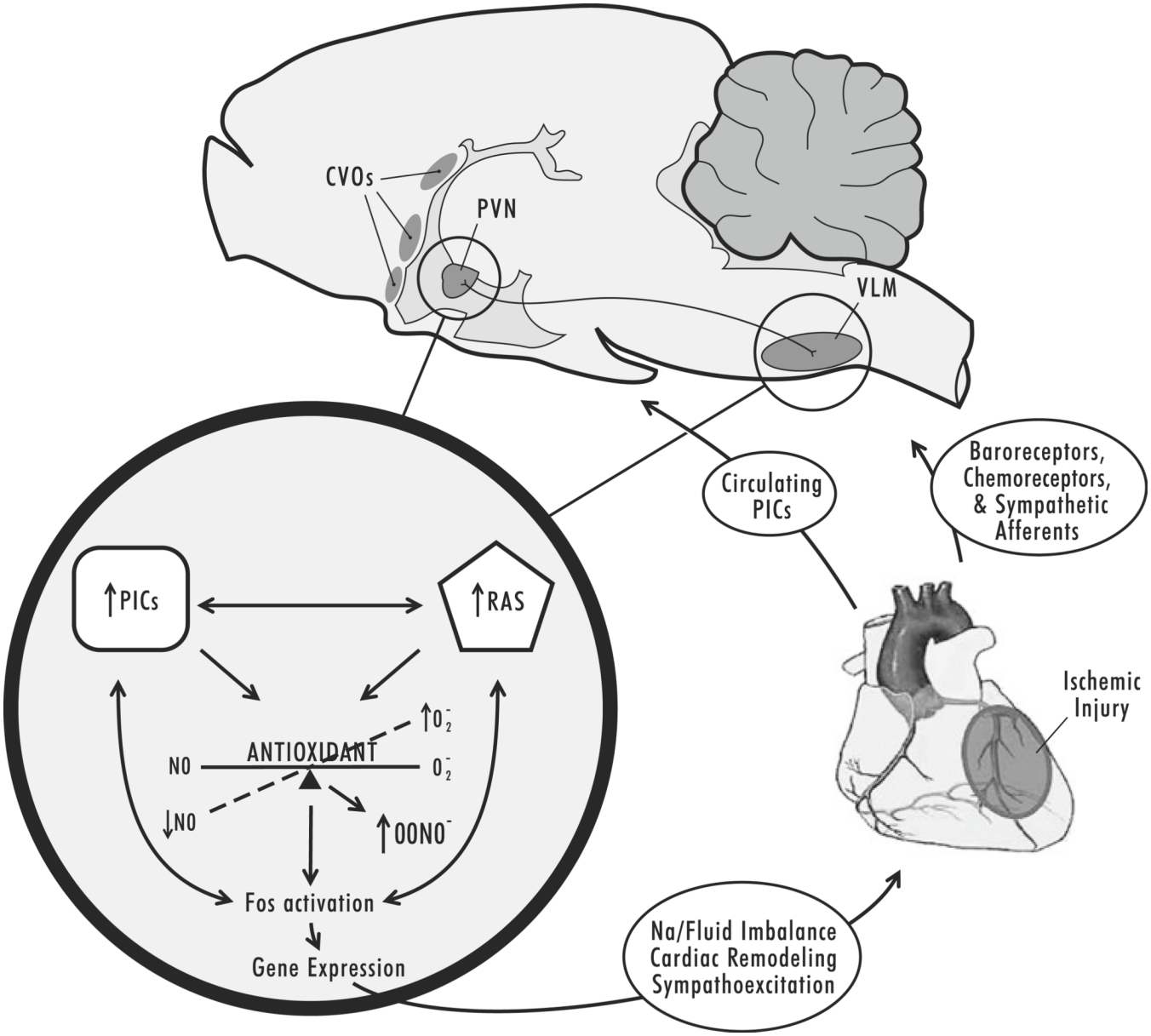

Fig. 7.

An illustration summary of our results. PICs released from the site of ischemic injury in the heart enter the CVOs through the circulation, and are subsequently carried/signal to the PVN and VLM, causing release of additional PICs and neurohormones. These molecules further lead to an imbalance of superoxide and NO and activate the c-Jun/JNK/c-Fos pathway and alter gene expression, ultimately resulting in enhanced sympathoexcitation and adverse cardiac remodeling

Table 1

Echocardiographic and morphologic findings in mice from protocols I and II

	PROTOCOL I						PROTOCOL II					
	WT + Sham/VEH		WT MI + VEH		WT MI + ETN		WT + MI		TNF KO + Sham		TNF KO + MI	
	24 h	4 weeks	24 h	4 weeks	24 h	4 weeks	24 h	4 weeks	24 h	4 weeks	24 h	4 weeks
n	15	15	11	8	10	9	48	37	15	15	45	42
B.Wt.	23 ± 0.8	24.9 ± 1.2	22.8 ± 0.9	24.3 ± 1.7	23.2 ± 1.0	24.6 ± 1.3	22.9 ± 0.6	24.1 ± 1.2	21.7 ± 0.9	23.4 ± 1.2	22 ± 1.1	23.8 ± 0.8
Echocardiographic parameters												
IVSS	1.33 ± 0.03	1.41 ± 0.02	1.32 ± 0.01	1.43 ± 0.04*	1.37 ± 0.06	1.35 ± 0.13	1.28 ± 0.08	1.39 ± 0.05*	1.31 ± 0.08	1.33 ± 0.02	1.34 ± 0.08	1.36 ± 0.06
IVSD	0.84 ± 0.03	0.87 ± 0.05	0.81 ± 0.04	0.84 ± 0.04	0.82 ± 0.04	0.83 ± 0.06	0.79 ± 0.02	0.81 ± 0.07	0.76 ± 0.03	0.78 ± 0.02	0.79 ± 0.03	0.81 ± 0.04
LVS	2.62 ± 0.06	2.63 ± 0.08	2.85 ± 0.04	3.79 ± 0.12*	2.87 ± 0.19	2.69 ± 0.12	2.87 ± 0.04	3.58 ± 0.13*	2.51 ± 0.16	2.49 ± 0.11	2.62 ± 0.06	2.70 ± 0.11
LVD	4.17 ± 0.11	4.22 ± 0.15	4.11 ± 0.08	4.76 ± 0.12*	4.17 ± 0.02	4.27 ± 0.07	4.17 ± 0.07	4.61 ± 0.08*	3.98 ± 0.17	4.02 ± 0.16	4.16 ± 0.13	4.26 ± 0.15
PWS	1.23 ± 0.07	1.27 ± 0.06	1.34 ± 0.07	1.41 ± 0.04*	1.24 ± 0.06	1.26 ± 0.10	1.19 ± 0.07	1.34 ± 0.08*	1.25 ± 0.07	1.26 ± 0.07	1.28 ± 0.06	1.31 ± 0.06
PWD	0.75 ± 0.07	0.77 ± 0.04	0.82 ± 0.07	0.84 ± 0.05	0.78 ± 0.05	0.76 ± 0.09	0.78 ± 0.05	0.81 ± 0.08	0.79 ± 0.04	0.80 ± 0.06	0.76 ± 0.04	0.74 ± 0.04
%FS	37.3 ± 1.83	37.6 ± 0.24	30.6 ± 0.45	20.5 ± 0.70**	30.9 ± 0.47	37.2 ± 1.10*	31.1 ± 1.06	22.5 ± 0.79*	37.1 ± 0.45	38.6 ± 0.32	36.9 ± 0.48	36.7 ± 1.01
%IZ	N/A	N/A	44.5 ± 2.3	47.6 ± 3.1	45.7 ± 3.2	48.6 ± 3.4	44.6 ± 2.9	47.2 ± 3.3	N/A	N/A	42.8 ± 2.8	45.6 ± 2.3
Morphological parameters												
HW/BW	N/A	4.33 ± 0.25	N/A	4.52 ± 0.05	N/A	4.29 ± 0.26	N/A	4.54 ± 0.18	N/A	4.21 ± 0.11	N/A	4.24 ± 0.13
LW/BW	N/A	4.61 ± 0.07	N/A	6.57 ± 0.36**	N/A	4.49 ± 0.30	N/A	5.55 ± 0.34*	N/A	4.31 ± 0.13	N/A	4.36 ± 0.16

Data presented are mean ± SEM

B.Wt (gm), body weight; *IVD* and *IVS* (mm), left ventricular internal diameter at end-systole and end-diastole, respectively; *LVD* and *LVS* (mm), left ventricular septal thickness at end-diastole and end-systole, respectively; *PWD* and *PWS* (mm), posterior wall thickness at end-diastole and end-systole, respectively; %*FS*, fractional shortening; %*IZ*, percent ischemic zone (* $p < 0.05$, ** $p < 0.01$ vs. 24 h MI); *HW/BW*, heart weight/body weight ratio; *LW/BW*, lung weight/body weight ratio.

* $p < 0.05$,

** $p < 0.01$ compared to respective sham group

Table 2

Gene data expressed relative to respective Sham values

Category	Transcript	Hypothalamus					Brainstem				
		WT + Sham	MI + VEH	MI + ETN	KO + Sham	KO + MI	WT + Sham	MI + VEH	MI + ETN	KO + Sham	KO + MI
n		8	10	8	8	10	8	10	8	8	10
Cytokines	TNF	1.04 ± 0.21	2.38 ± 0.09*	0.40 ± 0.34#	1.07 ± 0.23	0.88 ± 0.06	0.61 ± 0.09	2.01 ± 0.17	0.81 ± 0.85*	1.02 ± 0.12	1.15 ± 0.09
	IL-1β	1.26 ± 0.30	3.73 ± 0.06*	1.30 ± 0.45#	1.04 ± 0.17	1.52 ± 0.43	1.06 ± 0.13	2.81 ± 0.36*	1.96 ± 1.00	1.06 ± 0.22	1.39 ± 0.29*
	IL-6	1.12 ± 0.28	1.64 ± 0.11	1.08 ± 0.38	1.06 ± 0.19	0.96 ± 0.08	1.11 ± 0.20	1.38 ± 0.14	1.02 ± 0.31	1.04 ± 0.11	1.11 ± 0.18
	IL-10	1.08 ± 0.17	1.11 ± 0.08	4.31 ± 1.96*,#	1.06 ± 0.24	3.13 ± 0.66*	1.05 ± 0.11	0.53 ± 0.03	2.21 ± 1.71*	1.07 ± 0.19	1.01 ± 0.13
Nitric oxide synthases	nNOS	1.19 ± 0.41	0.59 ± 0.09*	1.27 ± 0.22#	1.40 ± 0.47	1.84 ± 0.11	1.14 ± 0.32	0.69 ± 0.09*	1.26 ± 0.42#	1.03 ± 0.14	1.66 ± 0.36
	eNOS	1.19 ± 0.40	0.90 ± 0.10	1.20 ± 0.05*	1.04 ± 0.16	1.94 ± 0.25*	1.15 ± 0.34	1.07 ± 0.07	1.26 ± 1.13	1.06 ± 0.21	1.76 ± 0.20*
	iNOS	0.92 ± 0.11	2.57 ± 0.12*	0.98 ± 0.06#	1.08 ± 0.25	0.75 ± 0.05	0.58 ± 0.03	0.90 ± 0.19	1.24 ± 0.16*	1.04 ± 0.17	0.63 ± 0.06*
Nox homologs	Nox2	1.12 ± 0.25	3.08 ± 0.38*	1.84 ± 0.33#	1.03 ± 0.13	1.21 ± 0.24	1.22 ± 0.46	1.96 ± 0.25	1.88 ± 0.23	1.01 ± 0.08	0.80 ± 0.17
	Nox4	1.17 ± 0.39	1.58 ± 0.15	0.99 ± 0.08	1.01 ± 0.08	0.84 ± 0.12	1.38 ± 0.66	1.28 ± 0.11	1.03 ± 0.07	1.01 ± 0.07	0.78 ± 0.04
AngII receptors	AT1R	1.07 ± 0.24	1.96 ± 0.19*	0.92 ± 0.12#	1.03 ± 0.16	0.64 ± 0.09	1.04 ± 0.31	1.79 ± 0.0*	1.04 ± 0.16#	1.04 ± 0.18	0.76 ± 0.03
	AT2R	1.18 ± 0.38	0.86 ± 0.09	1.56 ± 0.04	1.03 ± 0.14	1.97 ± 0.26*	1.13 ± 0.35	0.81 ± 0.09	1.28 ± 1.17	1.29 ± 0.44	1.42 ± 0.07

Values expressed are means ± SEM of relative gene expression ($2^{-\Delta\Delta Ct}$) to respective sham group with sham values arbitrarily set at 1.

* $p < 0.05$ as compared to respective sham group,

# $p < 0.05$ as compared to MI + VEH group